Magneto-photon-phonon interaction in a parabolically confined quantum dot in the presence of high magnetic fields and intense terahertz radiation fields

W. Y. Wang[1] and W. Xu[1,2,*]

[1]*Key Laboratory of Materials Physics, Institute of Solid State Physics, Chinese Academy of Sciences, Hefei 230031, China*

[2]*Department of Physics, Yunnan University, Kunming 650091, China*

(Received 5 February 2012; revised manuscript received 17 June 2012; published 9 July 2012)

We present a theoretical study on magneto-photon-phonon interaction in a parabolically confined quantum dot subjected simultaneously to static magnetic field and radiation field. A nonperturbative treatment for electron-photon interaction is proposed by solving analytically the time-dependent Schrödinger equation in which the magnetic field and the radiation field are included exactly. We employ the energy-balance equation approach on the basis of the Boltzmann equation to evaluate the energy transfer rate induced by optical transition events. It is found that for relatively low radiation levels, two peaks of the cyclotron resonance (CR) appear at two Kohn's frequencies $\omega_\pm$, and the strength and the width of the CR increase with radiation intensity. The CR at ω_+ is more prominent than that at ω_-. When the radiation become intense, the splitting of the CR peaks can be observed and the splitting increases with radiation intensity. The physics reasons behind these interesting findings are discussed. This study is pertinent to the application of intense terahertz radiation sources such as free-electron lasers in the investigation into low-dimensional semiconductor systems.

DOI: 10.1103/PhysRevB.86.045307 PACS number(s): 78.67.Hc, 78.20.Ls

I. INTRODUCTION

With the development of the nanogrowth and nanofabrication techniques, such as molecular beam epitaxy (MBE), metalorganic vapor phase epitaxy (MOVPE), droplet epitaxy based on self-assembly, etc., it has become possible to realize semiconductor-based quantum dot (QD) systems. In a QD the conducting electrons are confined within the nanometer distance scale comparable to the de Broglie wavelength so that the quantum effect can be observed and novel quantum phenomena can be measured experimentally. Semiconductor-based QD systems have been widely applied as advanced electronic and optoelectroic devices such as QD laser,[1] quantum cryptography,[2] quantum computer,[3] and memory chip,[4] to mention but a few. As a result, the theoretical and experimental investigation into electronic and optical properties of QDs has been an important and active field of research in condensed-matter physics, nanoelectronics, and optoelectronics. In particular, magneto-optical measurement has been a powerful experimental tool in the study and characterization of semiconductor QD systems.[5–13] When electrons in a QD are subjected to external magnetic field and light radiation, the applied fields can couple to the confining potential of the QD and the fields can couple with each other. Thus, the modified cyclotron resonance (CR) can be observed where the frequencies of the CR are comparable to the strength of the electronic correlations in the device systems. It is known that the transition energy for the dipole-allowed channels among the Fock-Darwin energy levels in a parabolically confined QD in the presence of a normal magnetic field is[6,11–13]

$$\Delta E = \hbar\omega_\pm \text{ with } \omega_\pm = \sqrt{\omega_0^2 + \frac{\omega_c^2}{4}} \pm \frac{\omega_c}{2}. \tag{1}$$

Here ω_0 is the characteristic frequency of a parabolically confined QD and $\omega_c = eB/m^*$ is the cyclotron frequency with B being the strength of the magnetic field and m^* the electron effective mass. The accuracy of this analytical expression has been carefully examined by variety of experiments.[5–9] In addition, published theoretical work[12,13] has given a distinct physical picture behind this simple and useful relation and has confirmed that two excitation frequencies ($\omega_\pm$) (also called Kohn's frequencies) from a parabolically confined QD are independent of the electron-electron interaction and of the number of electrons in the system. Hence, the magneto-optical absorption peaks at $\omega_\pm$ observed experimentally have been widely applied to characterize the QD systems and to measure the sample parameters such as the electron effective mass m^* and the strength of the confinement of the QD ω_0.

On the other hand, it is known that in the magneto-optical measurement, generally the sample and material-related parameters such as the scattering mechanisms[14,15] and the spin g factor, etc., affect mainly the amplitude and width of the magneto-optical absorption spectrum in an electron gas system. The phonon-assisted CR effect has been intensively studied in bulk[16–18] and two-dimensional (2D) semiconductor[19,20] systems. However, it has been found experimentally that when the radiation field becomes intense in the magneto-optical measurements, the splitting of the CR can be observed in bulk[21,22] and 2D[23] electron gas systems. In this study, we would like to see if we can observe the similar effect in QD systems in the magneto-optical experiments. At present, the intense terahertz (10^{12} Hz or THz) laser radiation can be generated through, for example, free-electron lasers (FELs).[24] The splitting of the CR peaks in GaAs-based two-dimensional electron gas (2DEG) systems have been experimentally measured using FELIX FELs.[23] Therefore, it has now become possible to examine how electrons in a QD response to intense THz laser radiation and quantizing magnetic field.

The theoretical investigation into magneto-optical properties of QDs is an old and well-documented problem. However, in the previous theoretical approaches, the radiation field has been often taken as a perturbation. When the radiation field becomes intense, such an approach may not be held. Thus, there is a need to develop nonperturbative theory to study electron interactions with intense radiation fields for QD structures. In the present study, we intend contributing a theoretical work in handling magneto-photon-phonon interaction in a parabolically confined QD, in which the radiation field is included in a more exact way. Such a new approach is developed in Sec. II. In conjunction with magneto-optical measurements, in Sec. III we present the numerical results for magneto-optical properties of GaAs-based QD systems and discuss the effect of intense THz laser radiation on these properties. In addition, the main theoretical findings from this study are summarized in Sec. IV.

II. THEORETICAL APPROACHES

A. Electronic states

In this paper, we consider a typical QD whose growth direction is taken along the z axis with a confining potential $U(z)$ and the lateral confining potential in the xy plane is taken as $V(x,y)=(m^*\omega_0^2/2)(x^2+y^2)$, where ω_0 is the characteristic frequency of a parabolically confined QD and m^* is the electron effective mass. A static magnetic field B and an electromagnetic (EM) field are applied simultaneously along the z direction of the QD, where the radiation field A_t is polarized linearly in the xy plane (taken along the x direction). Under the usual dipole approximation, the vector potential of the radiation field is given as $A_t=\Theta(t)(F_0/\omega)\sin(\omega t)$, where $\Theta(x)$ is the unit-step function and F_0 and ω are, respectively, the electric field strength and the frequency of the applied EM field. In such a geometry, both vector potentials induced by the magnetic and radiation fields couple to the lateral confining potential of the QD and the vector potential of the radiation field couples to that of the magnetic field. As a result, the effect of the modified CR is observable in this configuration. The single-electron Hamiltonian to describe such a magneto-photon system can be written as

$$H_0(t)=\frac{[p_x-(1-\alpha)eBy+eA_t]^2+(p_y+\alpha eBx)^2}{2m^*}+\sigma g\mu_B B+\frac{m^*}{2}\omega_0^2(x^2+y^2)+\frac{p_z^2}{2m^*}+U(z). \quad (2)$$

Here, $p_x=-i\hbar\partial/\partial x$ is the momentum operator along the x direction, $\sigma=\pm1$ refers to different spin states, g is the spin g factor, and μ_B is the Bohr magneton. To show how the results depend on the choice of the gauge for the magnetic field, here we use an arbitrary gauge for the vector potential induced by the B field, that is, the gauge factor $\alpha=[0,1]$ here. It is known that in the presence of a linearly polarized EM field, if the results can be obtained in one particular gauge of the vector potential induced by the radiation field, the results in an arbitrary gauge can also be obtained through the gauge transformation. We find that (see Appendix) the influence of the magnetic and radiation fields on electron wave function is mainly achieved through shifting the coordinates and phases of the wave fucntion. The coordinate shifts do not depend on the gauge of the B field at all, whereas the phase shifts depend on what the gauge factor α is taken to be. Most importantly, it is found that the corresponding Schrödinger equation can be solved analytically and the time-dependent electron wave function is obtained as (see Appendix)

$$|n,\nu,t\rangle=\Psi_{n\nu}(\mathbf{R},t)=\Phi_{n\nu}(\mathbf{r},t)\psi_n(z), \quad (3)$$

where

$$\Phi_{n\nu}(\mathbf{r},t)=\frac{e^{im\theta}}{\sqrt{2\pi}}R_{mN}\left(\sqrt{(x+x_t)^2+(y+y_t)^2}/l_0\right)\times e^{im^*[(x+x_t)u_t+(y+y_t)v_t]/\hbar}e^{-i[E_{n\nu}t+\int^t d\tau f(\tau)]/\hbar}.$$

Here, $\nu=(\sigma Nm)$ refers to quantum numbers for states in the xy plane, $\mathbf{R}=(\mathbf{r},z)=(x,y,z)$, θ is the angle between $(x+x_t,y+y_t)$ and the x axis, $m=0,\pm1,\pm2,\ldots$, $N=0,1,2,\ldots$, and $l_0=(\hbar/m^*\Omega_0)^{1/2}$, with $\Omega_0=\sqrt{\omega_0^2+\omega_c^2/4}$ and $\omega_c=eB/m^*$ being the cyclotron frequency. The energy spectrum of the QD is

$$E_{n\nu}=[2N+1+|m|+m(\omega_c/2\Omega_0)]\hbar\Omega_0+\sigma g\mu_B B+\varepsilon_n, \quad (4)$$

which is a well-known result when the symmetry gauge $\alpha=1/2$ is taken. The wave function $\psi_n(z)$ and electronic subband energy ε_n are determined by a time-independent Schrödinger equation along the growth direction, which are not affected directly by the magnetic and radiation fields. In Eq. (3),

$$R_{mN}(x)=\frac{1}{l_0}\sqrt{\frac{2N!}{(N+|m|)!}}e^{-x^2/2}x^{|m|}L_N^{|m|}(x^2),$$

obtained by taking the symmetry gauge $\alpha=1/2$ with $L_N^m(x)$ being a Laguerre polynomial. The shifts of the coordinates are

$$x_t=r_0\cos(\omega t)-r_+\cos(\omega_+t)-r_-\cos(\omega_-t), \quad (4a)$$

and

$$y_t=r_1\sin(\omega t)-r_+\sin(\omega_+t)+r_-\sin(\omega_-t), \quad (4b)$$

which do not depend on the choice of the gauge for the vector potential of the B field. Here, $\omega_\pm=\Omega_0\pm\omega_c/2$, $r_0=(eF_0/m^*)(\omega^2-\omega_0^2)/[(\omega^2-\omega_+^2)(\omega^2-\omega_-^2)]$, $r_1=(eF_0/m^*)\omega\omega_c/[(\omega^2-\omega_+^2)(\omega^2-\omega_-^2)]$, and $r_\pm=(eF_0/2m^*\Omega_0)\omega_\pm/(\omega^2-\omega_\pm^2)$. The phase shifts are

$$u_t=-\dot{x}_t-(1-\alpha)\omega_c y_t-(eF_0/m^*\omega)\sin(\omega t) \quad (4c)$$

and

$$v_t=\alpha\omega_c x_t-\dot{y}_t, \quad (4d)$$

which depend on the gauge factor α. Furthermore,

$$f(t)=(m^*/2)\left[\dot{x}_t^2+\dot{y}_t^2+2\dot{x}_t u_t+2\dot{y}_t v_t+\omega_0^2\left(x_t^2+y_t^2\right)\right] \quad (4e)$$

depends also on the gauge factor α. Here, $x_t=y_t=u_t=v_t=0$ at $t=0$ have been taken as initial conditions. We note that although the electron wave function given by Eq. (3) continues over all $\mathbf{R}$, t, and ω, the coordinate and phase shifts are divergent when $\omega\to\omega_\pm$. This implies that due to the coupling between the vector potentials of the magnetic and radiation fields and the lateral confinement potential of the QD, the CR can be achieved with two CR frequencies $\omega_\pm$, which is independent of the number of electrons in the dot. Hence, two Kohn's frequencies $\omega_\pm=\Omega_0\pm\omega_c/2$ are also the CR frequencies for a parabolically confined

QD subjected to magnetic and radiation fields. In such an approach, the radiation field can be included exactly within the time-dependent electron wave function. This can provide a basis for studying more easily the magneto-optical properties of a QD system.

B. Magneto-photon-phonon interaction

With time-dependent electron wave function given as Eq. (3), we can derive the retarded Green's function for electrons in the $(\mathbf{R},t)$ representation

$$G_0(\mathbf{R},t;\mathbf{R}',t') = \frac{\Theta(t-t')}{i\hbar}\sum_{n,\nu}\Psi^*_{n\nu}(\mathbf{R}',t')\Psi_{n\nu}(\mathbf{R},t),$$

which is a two-time quantity and satisfies

$$[i\hbar\partial/\partial t - H_0(t)]G_0(\mathbf{R},t;\mathbf{R}',t') = \delta(\mathbf{R}-\mathbf{R}')\delta(t-t').$$

Applying the Green's function approach to the time-dependent perturbation theory, in the presence of a scattering potential $V(\mathbf{R},t)$, the first-order contribution to the steady-state electronic transition rate can be calculated by[23]

$$W(\lambda';\lambda) = \frac{1}{\hbar^2}\lim_{t\to+\infty}\frac{\partial|G_{\lambda'\lambda}(t)|^2}{\partial t}, \tag{5}$$

where λ is the quantum number to describe the system and $G_{\lambda'\lambda}(t) = \int_0^t d\tau\langle\lambda',\tau|V(\mathbf{R},\tau)|\lambda,\tau\rangle$ with $|\lambda,t\rangle$ being the time-dependent electron wave function with regarding to $H_0(t)$.

In the present study, we consider polar semiconductor-based QD structures in which optic-phonon scattering is the limiting factor to determine the electronic and optical properties of the sample device at relatively high temperatures. We assume that the system under study can be separated into the electrons of interest and the rest of the crystal. For the case of electron interactions with bulklike phonons in a QD, the interaction Hamiltonian takes a form

$$V_{ep}(\mathbf{R},t) = \sum_{\mathbf{Q}}[V_{\mathbf{Q}}a_{\mathbf{Q}}e^{i(\mathbf{Q}\cdot\mathbf{R}+\omega_Q t)} + V^*_{\mathbf{Q}}a^\dagger_{\mathbf{Q}}e^{-i(\mathbf{Q}\cdot\mathbf{R}+\omega_Q t)}], \tag{6}$$

where $\mathbf{Q} = (\mathbf{q},q_z) = (q_x,q_y,q_z)$ is the phonon wave vector, $(a^\dagger_{\mathbf{Q}},a_{\mathbf{Q}})$ are the canonical conjugate coordinates of the phonon system, $V_{\mathbf{Q}}$ is the electron-phonon interaction coefficient, and ω_Q is the phonon frequency. After introducing the time-dependent electron wave function [Eq. (3)] and scattering potential for electron-phonon coupling [Eq. (6)] into Eq. (5), the first-order contribution to the steady-state electronic transition rate induced by magneto-photon-phonon scattering in a QD is obtained as

$$\begin{aligned} W_\pm(n',\nu';n,\nu) &= \frac{2\pi}{\hbar}\sum_{\mathbf{Q}}\begin{bmatrix}N_Q\\N_Q+1\end{bmatrix}|V_{\mathbf{Q}}|^2R^2_{m'N'mN}(l_0q)G_{n'n}(q_z)\\ &\times\sum_{M=-\infty}^{\infty}J^2_{m_1}(\gamma_{\mathbf{q}})J^2_{m_2}(r_+q)J^2_{m_3}(r_-q)\delta[E_{n'\nu'}-E_{n\nu}\\ &\mp\hbar\omega_Q + m_1\hbar\omega + m_2\hbar\omega_+ + m_3\hbar\omega_-], \end{aligned} \tag{7}$$

which measures the probability for scattering of an electron from a state $|n',\nu'\rangle$ to a state $|n,\nu\rangle$ due to electron interactions with the magnetic and radiation fields and with phonons. Here, the upper (lower) case refers to absorption (emission) of a phonon, $N_Q = (e^{\hbar\omega_Q/k_BT}-1)^{-1}$ is the phonon occupation number, $G_{n'n}(q_z) = |\langle n'|e^{iq_zz}|n\rangle|^2$ is the form factor for electron-phonon interaction along the growth direction with $|n\rangle$ being the electron wave function along this direction, $\gamma_{\mathbf{q}} = \sqrt{(r_0q_x)^2+(r_1q_y)^2}$, and $J_M(x)$ is a Bessel function. Furthermore,

$$\begin{aligned} R_{m'N'mN}(y) &= 2\left[\frac{N!N'!}{(N+|m|)!(N'+|m'|)!}\right]^{1/2}\\ &\times\int_0^\infty dx e^{-x^2}x^{|m|+|m'|+1}L_N^{|m|}(x^2)\\ &\times L_{N'}^{|m'|}(x^2)J_{m'-m}(xy), \end{aligned}$$

which can be further simplified as

$$\begin{aligned} &R_{m'N'mN}(y)\\ &= [N!N'!(N+|m|)!(N'+|m'|)!]^{1/2}e^{-y^2/4}\\ &\times\sum_{n=0}^{N}\sum_{n'=0}^{N'}\frac{(-1)^{n+n'}L_p^{|m'-m|}(y/2)^{|m'-m|+2}p!}{n!(N-n)!(n+|m|)!n'!(N'-n')!(n'+|m'|)!}, \end{aligned}$$

where $p = (|m|+|m'|-|m-m'|)/2+n+n'$. In the presence of a radiation field, the electronic transition in a QD can be accompanied not only by the emission and absorption of phonons but also by the emission and absorption of photons and cyclotron excitations. In Eq. (7), $m_1>0$, $m_1<0$, and $m_1=0$ correspond, respectively, to m_1-photon emission, m_1-photon absorption, and elastic-photon scattering. Similarly, $m_2>0$ ($m_3>0$), $m_2<0$ ($m_3<0$), and $m_2=0$ ($m_3=0$) correspond, respectively, to multicyclotron emission, absorption, and elastic cyclotron scattering with a transition energy $m_2\hbar\omega_+$ ($m_3\hbar\omega_-$). The corresponding Bessel functions in Eq. (7) play the roles in switching different photon and cyclotron scattering processes. In the absence of the radiation field (i.e., $F_0=0$), due to $\lim_{x\to0}J_M(x) = \delta_{M,0}$, we have

$$\begin{aligned} W_\pm(n',\nu';n,\nu) &= \frac{2\pi}{\hbar}\sum_{\mathbf{Q}}\begin{bmatrix}N_Q\\N_Q+1\end{bmatrix}|V_{\mathbf{Q}}|^2R^2_{m'N'mN}(l_0q)\\ &\times G_{n'n}(q_z)\delta[E_{n'\nu'}-E_{n\nu}\mp\hbar\omega_Q], \end{aligned} \tag{8}$$

which is a well-known result obtained previously for electron-phonon coupling in a parabolically confined QD system.[25,26]

As has been implied in the Appendix in Ref. 23, the electron-phonon interaction is taken as a perturbation in the present study. It is known that in the absence of the radiation field, such an approach works quite well for studying the consequences due to electron-phonon coupling in parabolically confined QD systems in quantizing magnetic fields.[25,26] In the presence of light radiation, because the radiation field has been included within the Hamiltonian $H_0(t)$ in Eq. (2), one would expect that such a perturbative approach can work even better in investigating the magneto-optical properties in QDs in the presence of phonon scattering. In particular, in the presence of an intense radiation field, a strong electron-photon interaction can be achieved and, therefore, it is more valid in our approach to take electron-phonon coupling as a perturbation in deriving the electronic transition rate induced by phonon scattering.

C. Magneto-optical absorption

In this study, we employ a semiclassic Boltzmann equation as the governing transport equation to study the consequences of a QD subjected simultaneously to the magnetic and radiation fields. The steady-state Boltzmann equation for such a magneto-photon-phonon system can be written, for a degenerate statistics, as

$$0=\sum_{n',\nu'}\left[F^{n\nu}_{n'\nu'}W(n',\nu';n,\nu)-F^{n'\nu'}_{n\nu}W(n,\nu;n',\nu')\right],\qquad(9)$$

where $F^{n'\nu'}_{n\nu}=f(E_{n\nu})[1-f(E_{n'\nu'})]$ with $f(E_{n\nu})$ being the energy-distribution function (EDF) for an electron at a state $|n,\nu\rangle$. It should be noted that the effect of the radiation field has been included within the electronic transition rate. Thus, to avoid double counting the force term induced by the radiation field does not appear on the left-hand side of the Boltzmann equation. The Boltzmann equation shown as Eq. (9) with the electronic transition rate given as Eq. (7) is a complicated equation. Due mainly to the inelastic nature of phonon and photon scattering and to the energy conservation law during a scattering event, which can vary the energy in the EDF for an electron in a final state when electron energy in the EDF in an initial state is fixed [i.e., both $f(x)$ and $f(x+m_1\hbar\omega+m_2\hbar\omega_++m_3\hbar\omega_-\pm\hbar\omega_Q)$ are present in one equation], there is no simple and analytical solution for Eq. (9). One numerical way to solve such an equation may be through, for example, Monte Carlo simulation (MCS),[27] which is very CPU consuming. At present, no result from MCS has been reported for a QD in the presence of radiation and magnetic fields. In the present study, we employ the usual balance-equation approach to solve the problem. The advantage of the balance-equation approach is that one can detour the difficulties of solving the Boltzmann equation directly and the interested physical properties can be calculated approximately on the basis of the statistical energy-distribution functions.[28] In this study, we consider that the system is under THz light radiation and the radiation photon energy is far less than the band gap of the QD. Thus, the presence of the radiation does not vary the carrier density of the QD system. As a result, the mass-balance equation (or the rate equation) does not hold. Because all electronic states in a QD are quantized, there is no electronic momentum transfer in the system and, therefore, no momentum-balance equation for a QD. Hence, for the first moment the energy-balance equation (EBE) can be derived by multiplying $\sum_{n,\nu}E_{n\nu}$ to both sides of the Boltzmann equation. In doing so, we obtain

$$0=\sum_{n',\nu',n,\nu}[E_{n'\nu'}-E_{n\nu}]F^{n'\nu'}_{n\nu}W(n,\nu;n',\nu')].\qquad(10)$$

Generally, the energy of a time-dependent state given as Eq. (3) is time-dependent, which can be obtained as $\mathbb{E}(t)=\langle\Psi_{n\nu}(\mathbf{r},t)|i\hbar\partial/\partial t|\Psi_{n\nu}(\mathbf{r},t)\rangle=E_{n\nu}+m^*[\dot{x}_t^2+\dot{y}_t^2+\omega_0^2(x_t^2+y_t^2)]/2$. For a steady-state, the static energy for an electron in a QD is $\mathbb{E}=(\omega/2\pi)\int_0^{2\pi/\omega}dt\mathbb{E}(t)=E_{n\nu}+E_s$ with $E_s=m^*[r_\pm^2(\omega_\pm^2+\omega_0^2)+(\omega_0^2+\omega^2)(r_0^2+r_1^2)/2]/2+m^*r_\pm\omega[r_0\omega_\pm(\omega^2+\omega_0^2)\pm r_1\omega(\omega_\pm^2+\omega_0^2)]\sin(2\pi\omega_\pm/\omega)/[\pi(\omega^2-\omega_\pm^2)]$ being the energy shift induced by the radiation and magnetic fields, which is time independent and does not depend on the electronic state. Because the energy shift E_s does not affect the electronic transition, the bare energies of the Fock-Darwin states appear in the EBE given as Eq. (10). The balance equation approach is a powerful tool for investigating theoretically the transport, optical, and optoelectronic properties of electronic systems.[29] In particular, the energy-balance equation on the basis of the Boltzmann equation has been widely applied in studying the electron-energy-loss rate and the electronic energy transfer rate in electron gas systems.[30] Equation (10) results in a relation

$$P_{op}+P_{ph}-P_{cr}=0,\qquad(11)$$

where P_j is the electron energy-transfer rate due to different scattering mechanisms,

$$P_{cr}=\frac{2\pi}{\hbar}\sum_{\mathbf{Q},n',\nu',n,\nu,M}(m_2\hbar\omega_++m_3\hbar\omega_-)\begin{bmatrix}N_Q\\N_Q+1\end{bmatrix}F^{n'\nu'}_{n\nu}\times|V_{\mathbf{Q}}|^2R^2_{m'N'mN}G_{n'n}(q_z)J^2_{m_1}(\gamma_{\mathbf{q}})J^2_{m_2}(r_+q)J^2_{m_3}(r_-q)\times\delta[E_{n'\nu'}-E_{n\nu}\mp\hbar\omega_Q+m_1\hbar\omega+m_2\hbar\omega_++m_3\hbar\omega_-]\qquad(12)$$

is induced by cyclotron excitation,

$$P_{op}=\frac{2\pi}{\hbar}\sum_{\mathbf{Q},n',\nu',n,\nu,M}(-m_1\hbar\omega)\begin{bmatrix}N_Q\\N_Q+1\end{bmatrix}F^{n'\nu'}_{n\nu}\times|V_{\mathbf{Q}}|^2R^2_{m'N'mN}G_{n'n}(q_z)J^2_{m_1}(\gamma_{\mathbf{q}})J^2_{m_2}(r_+q)J^2_{m_3}(r_-q)\times\delta[E_{n'\nu'}-E_{n\nu}\mp\hbar\omega_Q+m_1\hbar\omega+m_2\hbar\omega_++m_3\hbar\omega_-]\qquad(13)$$

is induced by electron-photon scattering, and

$$P_{ph}=P^+_{ph}-P^-_{ph}$$

is induced by electron-phonon scattering, which is the difference between phonon emission and absorption, with

$$P^\pm_{ph}=\frac{2\pi}{\hbar}\sum_{\mathbf{Q},n',\nu',n,\nu,M}\hbar\omega_Q\begin{bmatrix}N_Q\\N_Q+1\end{bmatrix}F^{n'\nu'}_{n\nu}|V_{\mathbf{Q}}|^2\times R^2_{m'N'mN}(l_0q)G_{n'n}(q_z)J^2_{m_1}(\gamma_{\mathbf{q}})J^2_{m_2}(r_+q)J^2_{m_3}(r_-q)\times\delta[E_{n'\nu'}-E_{n\nu}\mp\hbar\omega_Q+m_1\hbar\omega+m_2\hbar\omega_++m_3\hbar\omega_-].\qquad(14)$$

Equation (11) reflects a fact that in the QD system, the energy gain induced by optical absorption is balanced by the energy loss caused by phonon emission and cyclotron excitation.

In the presence of the broadening of the scattering states, we have

$$\delta(\mathcal{E}_{n\nu})\to\frac{\Gamma_{n\nu}/\pi}{\mathcal{E}^2_{n\nu}+\Gamma^2_{n\nu}}=\frac{1}{2\pi}\int_{-\infty}^{\infty}dx\,e^{-\Gamma_{n\nu}|x|}e^{i\mathcal{E}_{n\nu}x},\qquad(15)$$

with $\Gamma_{n\nu}$ being the broadened width for a state $|n,\nu\rangle$. Thus, we can carry out the m_1, m_2, and m_3 summations in the above Eqs. (12)–(14) easily. In particular, for electron energy transfer rate induced by electron-photon interaction, we obtain

$$P_{op} = 4 \sum_{\mathbf{Q},n',\nu',n,\nu} \omega\gamma_{\mathbf{q}} \begin{bmatrix} N_Q \\ N_Q+1 \end{bmatrix} F_{n\nu}^{n'\nu'} |V_{\mathbf{Q}}|^2 G_{n'n}(q_z) \times R^2_{m'N'mN}(l_0 q) \int_0^\infty dx e^{-2\Gamma_{n\nu}x} I^{\mathbf{q}}_{100}(x) \times \sin\left(X^{n\nu}_{n'\nu'}\right)\cos(\hbar\omega x), \quad (16)$$

where $X^{n\nu}_{n'\nu'} = 2(E_{n'\nu'} - E_{n\nu} \mp \hbar\omega_Q)x$ and $I^{\mathbf{q}}_{ijk}(x) = J_i[2\gamma_{\mathbf{q}}\sin(\hbar\omega x)]J_j[2r_-q\sin(\hbar\omega_- x)]J_k[2r_+q\sin(\hbar\omega_+ x)]$. In this study, we use Eq. (16) to calculate the electron energy transfer rate (or optical energy transition rate) induced by the electron-photon coupling, which is proportional to the magneto-optical absorption coefficient.

D. LO-phonon scattering in a QD

For the case of electron interactions with longitudinal optical (LO) phonons in a polar semiconductor-based QD, we have (i) $\omega_Q \simeq \omega_{LO}$ the LO-phonon frequency in the long-wavelength range; (ii) $N_Q \simeq N_0 = (e^{\hbar\omega_{LO}/k_BT} - 1)^{-1}$; and (iii) the coupling coefficient is given by the Fröhlich Hamiltonian so that $|V_{\mathbf{Q}}|^2 = 4\pi\alpha_{LO} L_0 (\hbar\omega_{LO})^2/Q^2$, where α_{LO} is the electron−LO-phonon coupling constant and $L_0 = (\hbar/2m^*\omega_{LO})^{1/2}$ is the polar radius.

At present, an often-used technique to produce semiconductor-based QDs is through defining the QD in the 2DEG formed in, for example, an AlGaAs/GaAs heterojunction.[31–33] The lateral confinement in the xy plane is achieved by applying gate voltages on the quantum point contacts.[31–33] It has been shown experimentally that in such a QD device, the lateral confining potential in the relatively low-energy regime is parabolic.[33] The situation where only the lowest electronic subband is occupied by electrons in the heterojunction along the z direction is taken into consideration. We apply the usual triangular well approximation to model the confining potential normal to the interface of the AlGaAs/GaAs heterojunction.[34] Thus, the form factor $G_{00}(q_z)$ can be determined analytically. The energy transfer rate induced by electron-photon interaction in a QD can then be written as

$$P_{op} = \frac{\alpha_{LO} L_0 b\hbar\omega^2_{LO}}{\pi} \int_0^\infty dx e^{-2\Gamma x}\cos x \int_0^\infty dy X(y) \times Y(2y\sin x) J_0[2b_- y\sin(\Omega_- x)] J_0[2b_+ y\sin(\Omega_+ x)] \times \sum_{\nu,\nu'} F_{\nu\nu'} \begin{bmatrix} N_0\sin(X^-_{\nu'\nu}) \\ (N_0+1)\sin(X^+_{\nu'\nu}) \end{bmatrix} R^2_{m'N'mN}(l_0 by), \quad (17)$$

where $F_{\nu\nu'} = f(E_{0\nu})[1 - f(E_{0\nu'})]$, $\Gamma_\nu = \Gamma_{0\nu}/\hbar\omega$, $X^{\mp}_{\nu'\nu} = 2(E_{0\nu'} - E_{0\nu} \mp \hbar\omega_{LO})x/\hbar\omega$, $X(y) = y(8 + 9y + 3y^2)/(1 + y)^3$, $b_\pm = r_\pm b$, $\Omega_\pm = \omega_\pm/\omega$, $Y(x) = \int_0^{2\pi} d\varphi G(\varphi) J_1(xG(\varphi))$ with $G(\varphi) = b\sqrt{r_0^2\cos\varphi^2 + r_1^2\sin\varphi^2}$, and $b = [(48\pi m^* e^2/\kappa\hbar^2)(N_{\rm depl} + 11n_e/32)]^{1/3}$ defines the thickness $(3/b)$ of the triangular well with κ the dielectric constant and $N_{\rm depl}$ being the depletion charge density.

III. RESULTS AND DISCUSSIONS

The numerical results of this paper pertain to GaAs-based QD structures. In the calculations the material parameters are taken as (i) static dielectric constant $\kappa = 12.9$; (ii) effective-electron-mass ratio $m^*/m_e = 0.0665$, with m_e being the electron rest mass; (iii) electron−LO-phonon coupling constant $\alpha_{LO} = 0.068$; and (iv) LO-phonon energy $\hbar\omega_{LO} = 36.6$ meV. As for sample parameters, (i) the depletion charge density for an $Al_xGa_{1-x}/GaAs$ heterostructure based QD is taken as $N_{\rm depl} = 5 \times 10^{14}\,{\rm cm}^{-2}$; (ii) the areal electron density is taken as $n_e = 2 \times 10^{11}\,{\rm cm}^{-2}$; and (iii) the characteristic energy of a parabolically confined QD is taken to be $\hbar\omega_0 = 10$ meV.

In this study, the width of the broadened scattering states is assumed as $\Gamma_{n\nu} = \gamma$, which can be evaluated roughly via[34] $\gamma = \hbar\omega_c\sqrt{2/\pi\mu_0 B}$ with μ_0 being the electron mobility at $B \to 0$ and $T \to 0$. $\mu_0 \sim 100\,{\rm m}^2/{\rm Vs}$ can be taken from the experimental data. To our knowledge, at present little is known about how an intense radiation field affects the broadening of the scattering states. We therefore assume that the width of the broadened scattering states is proportional to the width of the Landau levels (LLs) in an AlGaAs/GaAs heterojunction. This assumption is made on based on the following. (i) The QD we are interested in here is defined in the 2DEG in the heterojunction. (ii) The width of the broadened LLs, namely γ given above, is induced by intralevel short-range impurity scattering processes and is calculated via self-consistent Born approximation.[34] Thus, the mobility $\mu_0 \sim n_I^{-1}$ is used to replace the impurity concentration n_I. (iii) A similar approach can be employed to calculate γ for a parabolically confined QD. Considering that the short-range impurities are in the 2DEG and including only intralevel impurity scattering, a similar result for γ can be obtained for a QD although slightly different B-field dependence can be expected due to the difference between LL energy in a 2DEG and the Fock-Darwin energy in a parabolically confined QD. The calculation of γ for a QD requires further theoretical work considerably. We therefore do not attempt it in the present study.

For model calculations we consider about ten electrons in a QD and take $T = 77$ K in all calculations. The Fermi energy of the system is determined by the condition of electron number conservation. It should be noted that in a QD defined in a 2DEG and realized by applying gate voltages on the quantum point contacts, the electron numbers in the QD can be tuned by the gate voltages.[32]

The influence of the radiation intensity ($I \sim F_0^2$) on the spectrum of electron energy transfer rate (or optical absorption spectrum) induced by electron-photon scattering at a fixed magnetic field is shown in Fig. 1. Two resonance peaks appear at the Kohn's frequencies $\omega_\pm$ when radiation intensity $F_0 \leqslant 0.2$ kV/cm. Such a result is in agreement with previous theoretical calculations[12,13] for low-level light excitations. This indicates that the Kohn's frequencies $\omega_\pm$ are also the CR frequencies in this configuration and the presence of electron-phonon coupling does not affect the CR frequencies in a QD. Thus, the single-particle model is perfectly enough to describe magneto-optical absorption spectrum in such a magneto-photon-phonon system. With increasing radiation intensity, more interesting features can be observed when $\omega \sim \omega_\pm$. We

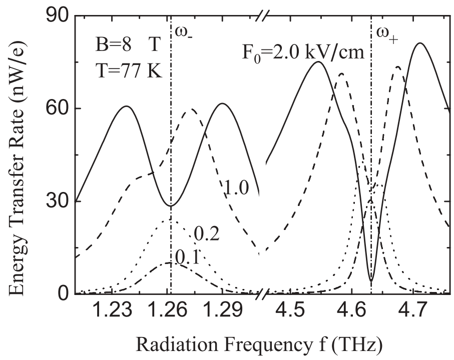

FIG. 1. Electron energy transfer rate per electron as a function of radiation frequency at a fixed magnetic field for different radiation intensities. Here the Kohn's frequencies, $\omega_\pm$, are shown to indicate the positions of the CR.

notice the following. (i) The amplitude and the width of the CR spectrum increase significantly with increasing radiation intensity when $F_0 \leqslant 0.2$ kV/cm. Meanwhile, the CR effect is more prominent at higher resonance frequency ω_+ compared with the lower one at ω_-. (ii) When $0.2 < F_0 < 1.0$ kV/cm, the splitting of the ω_+ CR peak can be seen and the splitting increases with radiation intensity. However, a similar splitting at lower resonance frequency ω_- cannot be observed. (iii) More interestingly, when $F_0 \geqslant 2.0$ kV/cm, both CR peaks at $\omega_\pm$ are simultaneously split and the splitting increases with increasing F_0.

Figure 2 shows the electron energy transfer rate as a function of magnetic field at a fixed radiation frequency for different radiation intensities. As can be seen, only one CR peak can been observed with varying B at a fixed ω. From the Kohn's frequencies $\omega_\pm$ and when $\omega \sim \omega_\pm$, we have $\omega_c = \pm(\omega^2 - \omega_0^2)/\omega$. Therefore, when fixing radiation frequency only one positive magnetic field corresponds to the CR peak. With increasing radiation intensity, the splitting of the CR peak can also be observed while varying the magnetic field.

Using Eq. (13), we can study the contribution from different optical transition channels to the total optical energy transfer rate (or optical absorption coefficient) for a QD in the presence of magnetic and radiation fields (see Figs. 3 and 4). In Fig. 3, we show contributions from $m_1 = \pm 1$ and ± 2 processes to optical

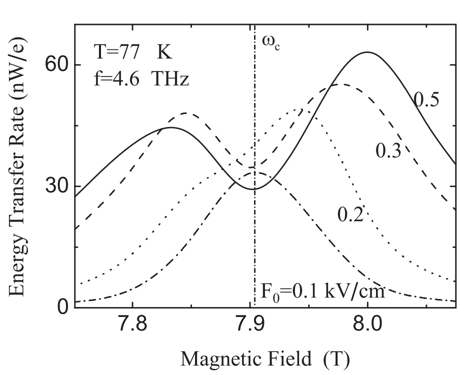

FIG. 2. Optical energy transfer rate per electron versus magnetic field at a fixed radiation frequency for different radiation intensities F_0, as indicated. Here the resonant frequency is at $\omega_c = |\omega^2 - \omega_0^2|/\omega$.

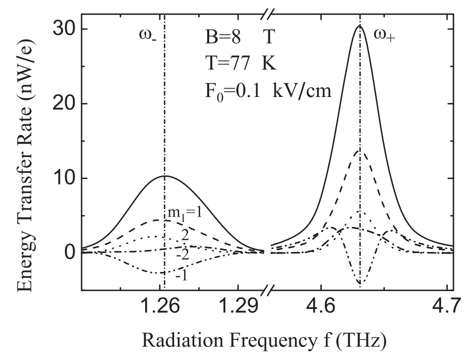

FIG. 3. Contributions from different photon emission ($m_1 < 0$) and absorption ($m_1 > 0$) channels to optical energy transfer rate per electron as a function of radiation frequency at the fixed radiation intensity F_0 and magnetic field B, as indicated. The total energy transfer rate is presented with the solid curve. The frequencies, $\omega_\pm$, are shown to indicate the positions of the CR.

energy transfer rate as a function of radiation frequency at a fixed radiation intensity and a fixed magnetic field. We note that $m_1 > 0$ and $m_1 < 0$ correspond respectively to m_1-photon absorption and m_1-photon emission channels. As can be seen, in the vicinity of resonant frequencies $\omega_\pm$, the contribution to the optical energy transfer rate can be achieved by electronic transitions via multiphoton absorption and emission channels. One can find that the contribution due to photon absorption channels (i.e., those associated with $m_1 > 0$) to optical energy transfer rate is much larger than that from photon emission channels (i.e., those with $m_1 < 0$). Away from the resonant regions, the optical transition is achieved mainly through one-photon absorption process. Furthermore, the optical energy transfer rate induced by the interaction with LO-phonons via photon emission ($m < 0$) is negative. A negative optical energy transfer rate means that the electrons in the system can gain the energy from the corresponding electronic transitions.

In addition, the dependence of the total electron energy transfer rate on the number of electrons in the QD is shown in Fig. 5. It has been demonstrated experimentally that in a QD defined in an AlGaAs/GaAs heterojunction and realized by applying the gate voltages on the quantum point contacts,

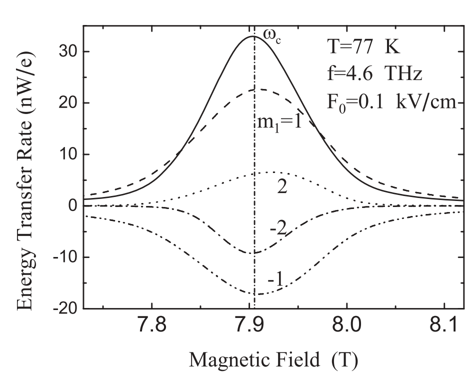

FIG. 4. Contributions from different photon absorption ($m_1 > 0$) and emission ($m_1 < 0$) channels to electron energy transfer rate per electron as a function of magnetic field at the fixed radiation frequency and intensity. The total energy transfer rate is shown with the solid curve. Here the resonant frequency is at ω_c.

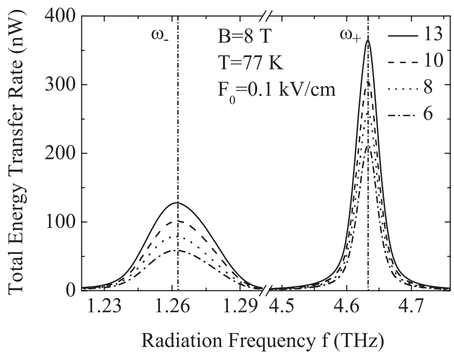

FIG. 5. Electron energy transfer rate as a function of radiation frequency at the fixed magnetic field and radiation intensity for different numbers of electrons in the QD, as indicated. The solid, dashed, dotted, and dash-dotted curves are for, respectively, 13, 10, 8, and 6 electrons in the QD. Here $\omega_\pm$ indicate the positions of the CR frequencies.

the electron numbers in the dot can be controlled by the gate voltages.[32] As can be seen, the positions of two peaks for magneto-optical absorption at the Kohn's frequencies $\omega_\pm$ do not change with varying the number of electrons in the QD. This confirms that the Kohn's frequencies are independent of the interactions among electrons and of the number of electrons in the QD, in line with the generalization of Kohn's theorem.[12,13] The number of electrons in the QD affects only the amplitude and width of the resonant peaks.

Now we discuss the physics reasons behind above-mentioned interesting and important features for a QD subjected to magnetic and radiation fields. (1) At relatively low radiation levels, that is, when $F_0 \leqslant 0.2$ kV/cm, the electrons in a QD can gain energy from the radiation field via photon absorption process. Because all energy states in a QD are quantized, photon absorption can lead to excitation of electrons from lower energy states below the Fermi level to higher energy levels above the Fermi level. In such a case, the excited electrons can lose the energy via emission of phonons and thus bring the electrons from higher-energy states back to lower-energy states. This two-step electronic transition processes can balance roughly the energy gain and loss in the electron-photon-phonon system. As a result, the CR can be achieved mainly via intralevel electronic transition channels in which the electrons gain the energy from the radiation field and lose the energy through excitation of the quanta $\hbar\omega_\pm$. Consequently, the peaks of the optical absorption (or optical energy transfer rate) can be observed when $\omega \sim \omega_\pm$. With increasing radiation intensity, the electron-photon scattering rate increases. Therefore, the intensity of CR effect increases with F_0 as shown in Fig. 1 when $F_0 \leqslant 0.2$ kV/cm for both $\omega \sim \omega_\pm$. (2) When the radiation field is intense enough (i.e., when $F_0 \geqslant 2.0$ kV/cm), the electrons in the QD can gain energy very quickly through photon absorption channels including multiphoton absorption mechanisms. Such a process can be much quicker than that achieved for electronic energy loss via electron-phonon scattering so that electrons gain more energy from radiation field than energy loss due to emission of phonons. Thus, two prime mechanisms can be present. First, the interlevel transitions can result in electrons running away from the system, i.e., the ionization of electrons from the QD. Our numerical results show that in this case, almost no electron is present the states below the Fermi level. Second, the electron energy loss is mainly achieved via CR effect occurred via intralevel excitations of quanta $\hbar\omega_\pm$. Such processes can lead to very strong electron-photon interaction when $\omega \sim \omega_\pm$. As a result, at two resonance frequency $\omega_\pm$, the effective electron-phonon scattering is suppressed and both CR peaks are simultaneously split. This is evident by the fact that the effect of CR peak splitting increases with increasing radiation intensity, as shown in Figs. 1 and 2. (3) Interestingly, at the intermediate radiation levels (i.e., when $0.2\ \mathrm{kV/cm} < F_0 < 2\ \mathrm{kV/cm}$), we have observed the splitting of the CR peak for ω_+ and the CR peak associated with ω_- is not well split (see Fig. 1). Because $\omega_+ > \omega_-$, a larger photon energy $\hbar\omega$ is required to observe the CR effect occurring at ω_+ than that to see the CR effect at ω_-. A larger photon energy implies a stronger effect of running away or ionization of electrons from the QD via interlevel transition events. Thus, the stronger effect of effective electron-photon interaction can be achieved at about $\omega \sim \omega_+$ through intralevel CR excitations. This is the main reason why at intermediate radiation levels the splitting of the CR peak can be observed for $\omega \sim \omega_+$ and not for $\omega \sim \omega_-$.

It is known that in polar-semiconductor-based QD systems, the strength of LO-phonon emission is much stronger than that of phonon absorption. Therefore, LO-phonon emission is the main mechanism for relaxation of photon excited electrons in the system. In the presence of intense radiation fields, the electron-photon interaction can be achieved via multiphoton emission and absorption channels (see Figs. 3 and 4). The processes of photon emission can lead to further energy loss for electrons in the system, which gives a negative optical energy transfer rate (see cases for $m < 0$ in Figs. 3 and 4). However, the overall strength for photon absorption is much stronger than that for photon emission, as shown in Figs. 3 and 4. Furthermore, the effect of multiphoton absorption or emission becomes weaker with increasing $|m|$. Therefore, our results indicate that one-photon absorption (i.e., the case for $m = 1$) is the main channel for electron-photon interaction in GaAs-based QDs when $F_0 \leqslant 2$ kV/cm.

It should be noted that the energy relaxation rate induced by electron-photon interaction can be evaluated through $1/\tau = P_{op}/\hbar\omega$. Our results show that τ is of the order of picosecond for a GaAs-based QD subjected to magnetic fields and THz radiation fields. Therefore, the condition $\omega\tau \sim 1$ can be satisfied for such a magneto-photon-phonon system. It implies that the intense THz radiation can modify strongly the process of electronic energy excitation and relaxation in the QD system, and this is the main reason why the interesting and important radiation effects can be observed.

It is worth mentioning that the similar splitting of the CR peak has been observed experimentally for bulk and 2D electronic systems.[21–23] The splitting of the CR peak was clearly observed experimentally in SiC-based structures[22] at relatively low-B fields when the microwave radiation power is larger than 100 mW at $T = 1.6$ K. Such effect was thought to be caused by the coupling of the electrons with LO-phonons and with intense microwave radiation. By applying the intense THz laser radiation generated by FELIX FELs, we have investigated both experimentally and theoretically the magneto-photon-phonon interaction in GaAs-based 2DEG systems through magneto-optical transport measurements in 2004.[23] The splitting of the CR peak in longitudinal resistivity ρ_{xx} was observed in high magnetic fields and relatively high temperatures $T = 150$ K when THz FEL radiation became intense. The theoretical findings shown in this paper are very similar to those observed in bulk and 2DEG systems. We therefore believe that the splitting of the peaks of the CR can also be observed in GaAs-based QD systems at relatively high temperatures by using THz FEL radiation.

In addition, for the first sight the splitting of the CR peaks observed in this study looks a bit similar to the Rabi splitting (RS) occurring in a QD in the presence of intense light radiation.[35,36] However, the RS takes place in a regime where $\Omega_R\tau \gg 1$. Here $\Omega_R = DF_0/\hbar$ is the Rabi frequency, with D being the transition dipole moment of a two-level system (TLS) induced by, for example, exciton[35] or charged exciton[36] in a QD, and τ is the corresponding relaxation or decay time. Hence, to be able to observe the RS effect the TLS has to be formed and the coupling strength or the Rabi frequency Ω_R should significantly exceed the decay rate of the system. In contrast, the splitting of the CR peaks shown here occurs under the condition $\omega\tau \sim 1$ and requires an intense radiation. Moreover, the RS is a signature of a strongly coupled TLS. Thus, the physical origin of the RS differs essentially from the splitting of CR peaks discussed in this paper.

IV. CONCLUSIONS

In this study, we have proposed a nonperturbative treatment to deal with electron interactions with static magnetic fields and intense radiation fields in parabolically confined QD systems. On this basis, we are able to study more easily the magneto-optical properties in this system in the presence of scattering centers such as phonons and impurities. We have applied the energy-balance equation approach derived from the Boltzmann equation to theoretically study the magneto-photon-phonon interaction in GaAs-based QD structures. The electron energy transfer rate induced by magneto-optical transition, which is proportional to magneto-optical absorption coefficient, has been calculated and discussed. The main conclusions obtained from the present study are summarized as follows.

For a parabolically confined QD subjected simultaneously to magnetic and radiation field, the time-dependent Schrödinger equation can be solved analytically where the radiation field can be included exactly. We find that the effect of the coupled magnetic and radiation fields on time-dependent electron wave function is through shifting the coordinates and phases. The coordinate shifts do not depend on the choice of the gauge for the magnetic field, whereas the phase shifts depend on the gauge factor of the magnetic field. Moreover, due to the coupling of the magnetic field and the radiation field and to the coupling of these fields to the confining potential of the QD, the time-dependent electron wave function diverges when $\omega \to \omega_\pm = \sqrt{\omega_0^2 + \omega_c^2/4} \pm \omega_c/2$. This suggests that when the radiation frequency ω is around the Kohn's frequencies $\omega_\pm$, the effect of CR can be observed in a parabolically confined QD in the presence of the magnetic field.

With the time-dependent electron wave function in which the magnetic and radiation fields have been considered exactly in a QD, we can derive the steady-state electronic transition rate induced by magneto-photon-phonon interaction using the Green's function technique. Thus, we are able to calculate more easily and more accurately the measurable physics properties induced by magneto-photon-phonon coupling in the corresponding device systems. On the basis of the energy-balance equation derived from the Boltzmann equation, we have calculated the electron energy transfer rate induced by magneto-optical transition events as the function of magnetic field and of the intensity and frequency of the radiation field. The theoretical approach developed in this paper has gone beyond the conventional way to deal with magneto-photon interaction in a QD. It is very useful and powerful to handle the case where the intense radiation is present so that it cannot be taken a perturbation.

We have found that at relative low radiation intensities, two CR peaks can be observed at the Kohn's frequencies as documented previously. In such a case, CR occurs via intralevel electronic excitations and the strength and the width of the CR peaks increase with radiation intensity. When the radiation intensity is strong enough, the splitting of the CR peaks can be observed. This is because the electrons in the system gain more energy from radiation field than lose it via phonon emission. As a result, the effective electron-phonon coupling is suppressed and the effective electron-photon interaction is enhanced. In this case, almost no electron is present in the states below the Fermi level. Consequently, the strong CR occurs via intralevel excitations. The splitting of the CR peaks increases with radiation intensity. Similar phenomena have been observed experimentally in bulk materials and in 2D electron gas systems.

We have demonstrated that the interesting CR in GaAs-based QD systems can be measured in the presence of intense THz radiation fields. Currently, THz FELs (e.g., UCSB and FELIX) have been applied to scientific investigation into various material systems including low-dimensional semiconductor structures. We therefore hope the theoretical findings discussed in this paper can be verified experimentally in the near feature.

ACKNOWLEDGMENTS

This work was supported by the National Natural Science Foundation of China (Grant No. 10974206), the Chinese Academy of Sciences, the Ministry of Science and Technology of China (Grant No. 2011YQ130018), and by the Department of Science and Technology of Yunnan Province.

APPENDIX

In this Appendix, we present a simple way to solve time-dependent Schrödinger equation with a Hamiltonian given by Eq. (2). Because the presence of the B and A_t fields does not affect the electronic states along the z direction, the solution of the corresponding Schrödinger equation is in a form

$$\Psi(\mathbf{R},t) = \Phi(x,y,t)\psi_n(z)e^{-i(\varepsilon_n+\sigma g\mu_B B)t/\hbar}, \quad \text{(A1)}$$

where the wave function $\psi_n(z)$ and electronic subband energy ε_n are determined by a time-independent Schrödinger equation along the z direction. The wave function $\Phi(x,y,t)$ satisfies

$$i\hbar\dot{\Phi}(x,y,t) = H_1(t)\Phi(x,y,t), \quad \text{(A2)}$$

with

$$H_1(t) = \frac{[p_x - (1-\alpha)eBy + eA_t]^2 + (p_y + \alpha eBx)^2}{2m^*} + \frac{m^*}{2}\omega_0^2(x^2+y^2).$$

Letting $X = x + x_t$ and $Y = y + y_t$, Eq. (A2) becomes

$$i\hbar\dot{\Phi}(X,Y,t) = [H_0^* + R(t) + S(t) + T(t)]\Phi(X,Y,t), \quad \text{(A3)}$$

where

$$H_0^* = \frac{[p_X - (1-\alpha)eBY]^2 + (p_Y + \alpha eBX)^2}{2m^*} + \frac{m^*}{2}\omega_0^2(X^2+Y^2),$$

$$R(t) = \frac{m^*}{2}\left\{\left[(1-\alpha)\omega_c y_t + \frac{eA_t}{m^*}\right]^2 + \alpha^2\omega_c^2 x_t^2 + \omega_0^2(x_t^2+y_t^2)\right\},$$

$$S(t) = [\dot{x}_t + (1-\alpha)\omega_c y_t + eA_t/m^*]p_X + (\dot{y}_t - \alpha\omega_c x_t)p_Y,$$

$$T(t) = -m^*[(1-\alpha)^2\omega_c^2 y_t + \omega_0^2 y_t + (1-\alpha)\omega_c eA_t/m^*]Y - m^*(\alpha^2\omega_c^2 + \omega_0^2)x_t X,$$

and $\omega_c = eB/m^*$ is the cyclotron frequency. Assuming $\Phi(X,Y,t) = e^{im^*(u_t X + v_t Y)/\hbar}e^{-i[\mathcal{E}t + \int^t d\tau\, f(\tau)]/\hbar}\phi(X,Y)$, we get that $\phi(X,Y)$ and $\mathcal{E}$ are determined by

$$(H_0^* - \mathcal{E})\phi(X,Y) = 0,$$
$$f(t) = \frac{m^*}{2}\left[\dot{x}_t^2 + \dot{y}_t^2 + 2\dot{x}_y u_t + 2\dot{y}_t v_t + \omega_0^2(x_t^2+y_t^2)\right], \quad \text{(A4)}$$

and x_t, y_t, u_t, and v_t are determined, respectively, by

$$\dot{x}_t + (1-\alpha)\omega_c y_t + u_t = -eA_t/m^*, \quad \text{(A5a)}$$
$$-\alpha\omega_c x_t + \dot{y}_t + v_t = 0, \quad \text{(A5b)}$$
$$-(\alpha^2\omega_c^2 + \omega_0^2)x_t + \dot{u}_t + \alpha\omega_c v_t = 0, \quad \text{(A5c)}$$

and

$$[(1-\alpha)^2\omega_c^2 + \omega_0^2]y_t + (1-\alpha)\omega_c u_t - \dot{v}_t = -(1-\alpha)\omega_c eA_t/m^*. \quad \text{(A5d)}$$

Equation (A5) can be solved through

$$[O^4 + 2(\omega_0^2 + \omega_c^2/2)O^2]x_t = -e(O^2+\omega_0^2)\dot{A}_t/m^*, \quad \text{(A6a)}$$
$$O^2 y_t + \omega_0^2 y_t - \omega_c\dot{x}_t = 0, \quad \text{(A6b)}$$
$$u_t = -\dot{x}_t - (1-\alpha)\omega_c y_t - eA_t/m^*, \quad \text{(A6c)}$$

and

$$v_t = \alpha\omega_c x_t - \dot{y}_t, \quad \text{(A6d)}$$

with $O = \partial/\partial t$. We note that the coordinate shifts x_t and y_t do not depend on the choice of gauge for the vector potential of the magnetic field, whereas the phase shifts u_t and v_t depend on the gauge of the vector potential induced by the B field.

For the case where time-dependent vector potential is induced by a linearly polarized radiation field, we have $A_t = \Theta(t)(F_0/\omega)\sin(\omega t)$ under the usual dipole approximation, where $\Theta(x)$ is the unit-step function and F_0 and ω are, respectively, the electric field strength and the frequency of the radiation field. Using the initial conditions under which $x_t = y_t = u_t = v_t = 0$ at $t = 0$, we have

$$x_t = r_0\cos(\omega t) - r_+\cos(\omega_+ t) - r_-\cos(\omega_- t), \quad \text{(A7a)}$$
$$y_t = \frac{\omega\omega_c r_0}{\omega^2 - \omega_0^2}\sin(\omega t) - r_+\sin(\omega_+ t) + r_-\sin(\omega_- t), \quad \text{(A7b)}$$

and u_t and v_t are obtained using, respectively, Eqs. (A6c) and (A6d). Here, $\omega_\pm = \Omega_0 \pm \omega_c/2$ with $\Omega_0 = \sqrt{\omega_0^2 + \omega_c^2/4}$, $r_0 = (eF_0/m^*)(\omega^2 - \omega_0^2)/[(\omega^2-\omega_+^2)(\omega^2-\omega_-^2)]$, and $r_\pm = (eF_0/2m^*\Omega_0)\omega_\pm/(\omega^2-\omega_\pm^2)$.

We know that it is convenient to solve Eq. (A4) in the symmetry gauge where the gauge factor $\alpha = 1/2$, which reads

$$\phi(X,Y) = \phi_{mN}(\mathcal{R},\theta) = (1/\sqrt{2\pi})e^{im\theta}R_{mN}(\mathcal{R}/l_0), \quad \text{(A8)}$$

and

$$\mathcal{E} = E_{mN} = [2N + 1 + |m| + m(\omega/2\Omega_0)]\hbar\Omega_0, \quad \text{(A9)}$$

where $m = 0,\pm1,\pm2,\ldots$, $N = 0,1,2,\ldots$, $\mathcal{R} = \sqrt{X^2+Y^2}$, θ is the angle between (X,Y) and the x axis, $l_0 = (\hbar/m^*\Omega_0)^{1/2}$, and

$$R_{mN}(x) = \frac{1}{l_0}\sqrt{\frac{2N!}{(N+|m|)!}}e^{-x^2/2}x^{|m|}L_N^{|m|}(x^2),$$

with $L_N^m(x)$ being a Laguerre polynomial. It should be noted that, in the above derivations, no assumption regarding the validity of Eq. (A4) has been made. Thus, Eq. (A4) must be completely equivalent to Eq. (A2). Consequently, the time-dependent electron wave function for a parabolically confined QD subjected to a static magnetic field and a linearly polarized EM feld is given by Eq. (3).

*wenxu_issp@yahoo.cn

[1]H. Saito, K. Nishi, I. Ogura, S. Sugou, and Y. Sugomito, Appl. Phys. Lett. **69**, 3140 (1996).
[2]S. N. Molotkov and S. S. Nazin, JETP Lett. **63**, 687 (1996).
[3]D. Loss and D. P. DiVincenzo, Phys. Rev. A **57**, 120 (1998).
[4]T. J. Thornton, Rep. Prog. Phys. **58**, 311 (1995).
[5]T. Chakraborty, Comments Cond. Mat. Phys. **16**, 35 (1992).
[6]T. Chakraborty, *Quantum Dots* (North-Holland, Amsterdam, 1999).

[7]I. Magnusdottir and V. Gudmundsson, Phys. Rev. B **60**, 16591 (1999).
[8]B. Meurer, D. Heitmann, and K. Ploog, Phys. Rev. Lett. **68**, 1371 (1992).
[9]T. Chakraborty, V. Halonen, and P. Pietiläinen, Phys. Rev. B **43**, 14289 (1991).
[10]P. Pietiläinen and T. Chakraborty, Phys. Rev. B **73**, 155315 (2006).
[11]C. Sikorski and U. Merkt, Phys. Rev. Lett. **62**, 2164 (1989).
[12]F. M. Peeters, Phys. Rev. B **42**, 1486 (1990).
[13]P. A. Maksym and T. Chakraborty, Phys. Rev. Lett. **65**, 108 (1990).
[14]T. Ohyama, K. Sakakibara, E. Otsuka, M. Isshiki, and K. Igaki, Phys. Rev. B **37**, 6153 (1988).
[15]M. A. Hopkins, R. J. Nicholas, D. J. Barnes, M. A. Brummell, J. J. Harris, and C. T. Foxon, Phys. Rev. B **39**, 13302 (1989).
[16]T. M. Rynne and H. N. Spector, J. Appl. Phys. **52**, 393 (1981).
[17]E. J. Johnson and D. M. Dickey, Phys. Rev. B **1**, 2676 (1970).
[18]R. C. Enck, A. S. Saleh, and H. Y. Fan, Phys. Rev. **182**, 790 (1969).
[19]J. S. Bhat, S. S. Kubakaddi, and B. G. Mulimani, J. Appl. Phys. **70**, 2216 (1991).
[20]J. S. Bhat, R. A. Nesargi, and B. G. Mulimani, Phys. Rev. B **73**, 235351 (2006).
[21]T. Tomaru, T. Ohyama, E. Otsuka, M. Isshiki, and K. Igaki, Phys. Rev. B **46**, 9390 (1992).
[22]B. K. Meyer, D. M. Hofmann, D. Volm, W. M. Chen, N. T. Son, and E. Janzén, Phys. Rev. B **61**, 4844 (2000).
[23]W. Xu, R. A. Lewis, P. M. Koenraad, and C. J. G. M. Langerak, J. Phys.: Condens. Matter **16**, 89 (2004).
[24]L.-H. Yu, M. Babzien, I. Ben-Zvi, L. F. Dimauro, A. Doyuran, W. Graves, E. Johnson, S. Krinsky, R. Malone, I. Pogorelsky, J. Skaritka, G. Rakowsky, L. Solomon, X. J. Wang, M. Woodle, V. Yakimenko, S. G. Biedron, J. N. Galayda, E. Gluskin, J. Jagger, V. Sajaev, and I. Vasserman, Science **289**, 932 (2000).
[25]K. D. Zhu and S. W. Gu, Phys. Rev. B **47**, 12941 (1993).
[26]R. Haupt and L. Wendler, Solid-State Electron. **37**, 1153 (1994).
[27]See, e.g., W. Xu, F. M. Peeters, and J. T. Devreese, Phys. Rev. B **43**, 14134 (1991); **46**, 7571 (1992).
[28]W. Xu and C. Zhang, Phys. Rev. B **55**, 5259 (1997).
[29]W. Xu, H. M. Dong, L. L. Li, J. Q. Yao, P. Vasilopoulos, and F. M. Peeters, Phys. Rev. B **82**, 125304 (2010); H. M. Dong, W. Xu, and F. M. Peeters, J. Appl. Phys. **110**, 63704 (2011).
[30]See, e.g., K. Seeger, *Semiconductor Physics: An Introduction* (Springer-Verlag, New York, 2004).
[31]See, e.g., J. M. Elzerman, R. Hanson, L. H. Willems van Beveren, L. M. K. Vandersypen, and L. P. Kouwenhoven, Appl. Phys. Lett. **84**, 4617 (2004).
[32]R. Hanson, L. P. Kouwenhoven, J. R. Petta, S. Tarucha, and L. M. K. Vandersypen, Rev. Mod. Phys. **79**, 1217 (2007).
[33]O. Astafiev, V. Antonov, T. Kutsuwa, and S. Komiyama, Phys. Rev. B **65**, 085315 (2002).
[34]T. Ando, A. B. Fowler, and F. Stern, Rev. Mod. Phys. **54**, 437 (1982).
[35]X. Xu, B. Sun, P. R. Berman, D. G. Steel, A. S. Bracker, D. Gammon, and L. J. Sham, Science **317**, 929 (2007).
[36]M. Kroner, C. Lux, S. Seidl, A. W. Holleitner, K. Karrai, A. Badolato, P. M. Petroff, and R. J. Warburton, Appl. Phys. Lett. **92**, 031108 (2008).